



---

## Figures and figure supplements

*Drosophila* neprilysins control insulin signaling and food intake via cleavage of regulatory peptides

**Benjamin Hallier et al**

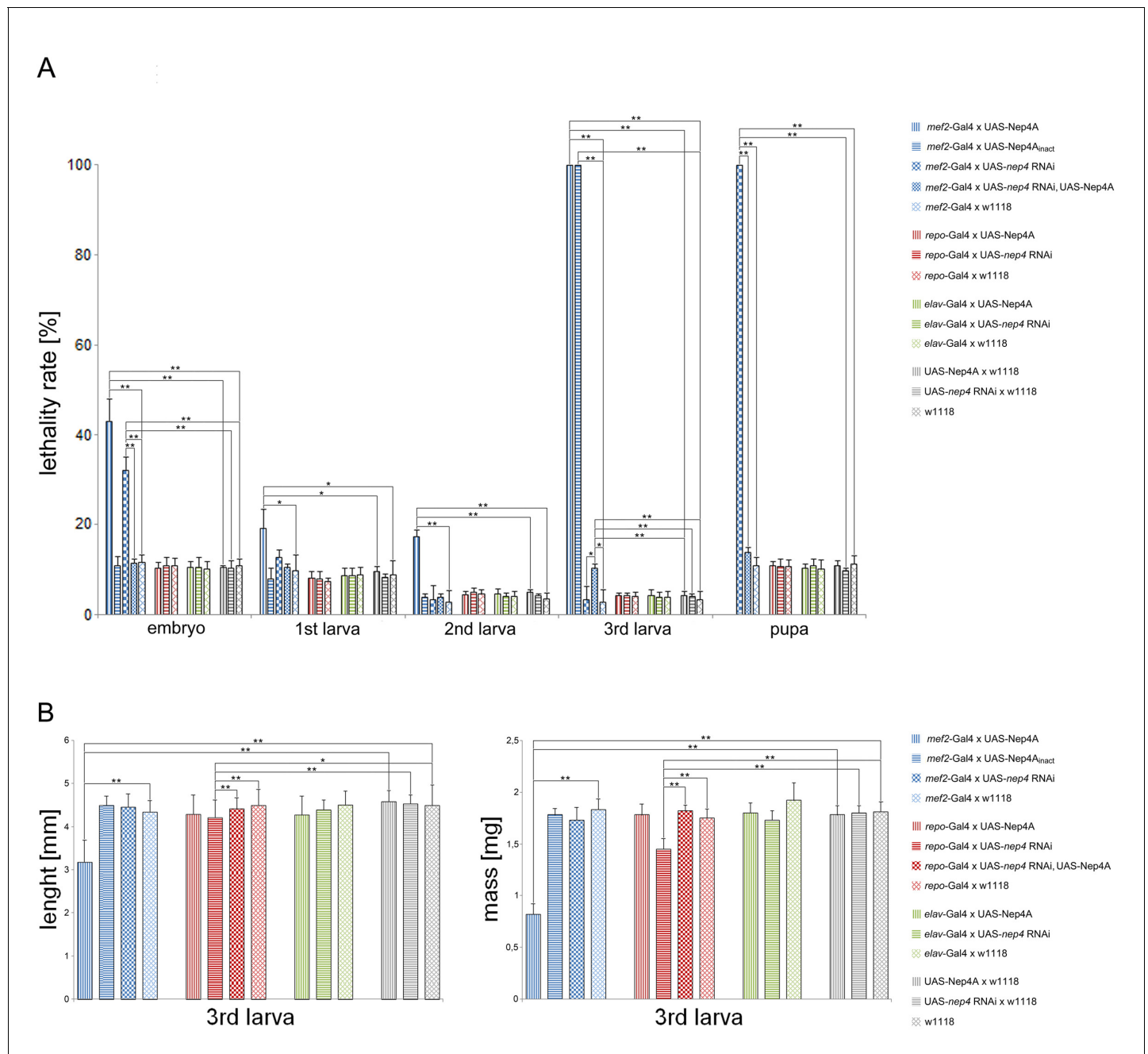


**Figure 1.** Modulating *nep4* expression affects life span and body size. **(A)** Lethality assay. The percentages (%) of animals of a specific stage that did not develop into the next stage are shown. While muscle-specific overexpression of Nep4A (*mef2-Gal4* x UAS-Nep4A) led to biphasic lethality with critical phases during embryonic and late larval development, overexpression of catalytically inactive Nep4A in the same tissue (*mef2-Gal4* x UAS-Nep4A<sub>inact</sub>) led to lethality only in the third instar larval stage. Muscle-specific *nep4* knockdown (*mef2-Gal4* x UAS-*nep4* RNAi) slightly increased embryonic lethality, but the majority of the animals died as pupae. Glial cell-specific overexpression of the peptidase (*repo-Gal4* x UAS-Nep4A) or knockdown of the peptidase (*repo-Gal4* x UAS-*nep4* RNAi) did not affect life span, which was also observed for neuronal overexpression or knockdown (*elav-Gal4* x UAS-Nep4A; *elav-Gal4* x UAS-*nep4* RNAi). *mef2-Gal4* x w1118, *repo-Gal4* x w1118, *elav-Gal4* x w1118, UAS-Nep4A x w1118, UAS-*nep4* RNAi x w1118, and w1118 were used as controls. Asterisks indicate statistically significant deviations from the respective controls (\* $p < 0.05$ , \*\* $p < 0.01$ , one-way ANOVA with pairwise comparisons). **(B)** Size and weight measurements. While muscle-specific overexpression of Nep4A (*mef2-Gal4* x UAS-Nep4A) reduced the size and wet mass of third instar larvae, neither overexpression of catalytically inactive Nep4A in the same tissue (*mef2-Gal4* x UAS-Nep4A<sub>inact</sub>) nor muscle-specific *nep4* knockdown (*mef2-Gal4* x UAS-*nep4* RNAi) significantly affected these parameters. Glial cell-specific overexpression of the peptidase (*repo-Gal4* x UAS-Nep4A) did not alter size or weight, while downregulation of the peptidase in the same tissue (*repo-Gal4* x UAS-*nep4* RNAi) slightly, but significantly, reduced both parameters. Neuronal overexpression or knockdown of *nep4* (*elav-Gal4* x UAS-Nep4A; *elav-Gal4* x UAS-*nep4* RNAi) had no effect on size or weight. Figure 1 continued on next page

Figure 1 continued

no effect on size or weight. Control lines were the same as in A. Asterisks indicate statistically significant deviations from respective controls (\* $p < 0.05$ , \*\* $p < 0.01$ , one-way ANOVA with pairwise comparisons).

DOI: [10.7554/eLife.19430.003](https://doi.org/10.7554/eLife.19430.003)

The following source data is available for figure 1:

**Source data 1.** Lethality assay.

DOI: [10.7554/eLife.19430.004](https://doi.org/10.7554/eLife.19430.004)

**Source data 2.** Size and weight measurements.

DOI: [10.7554/eLife.19430.005](https://doi.org/10.7554/eLife.19430.005)

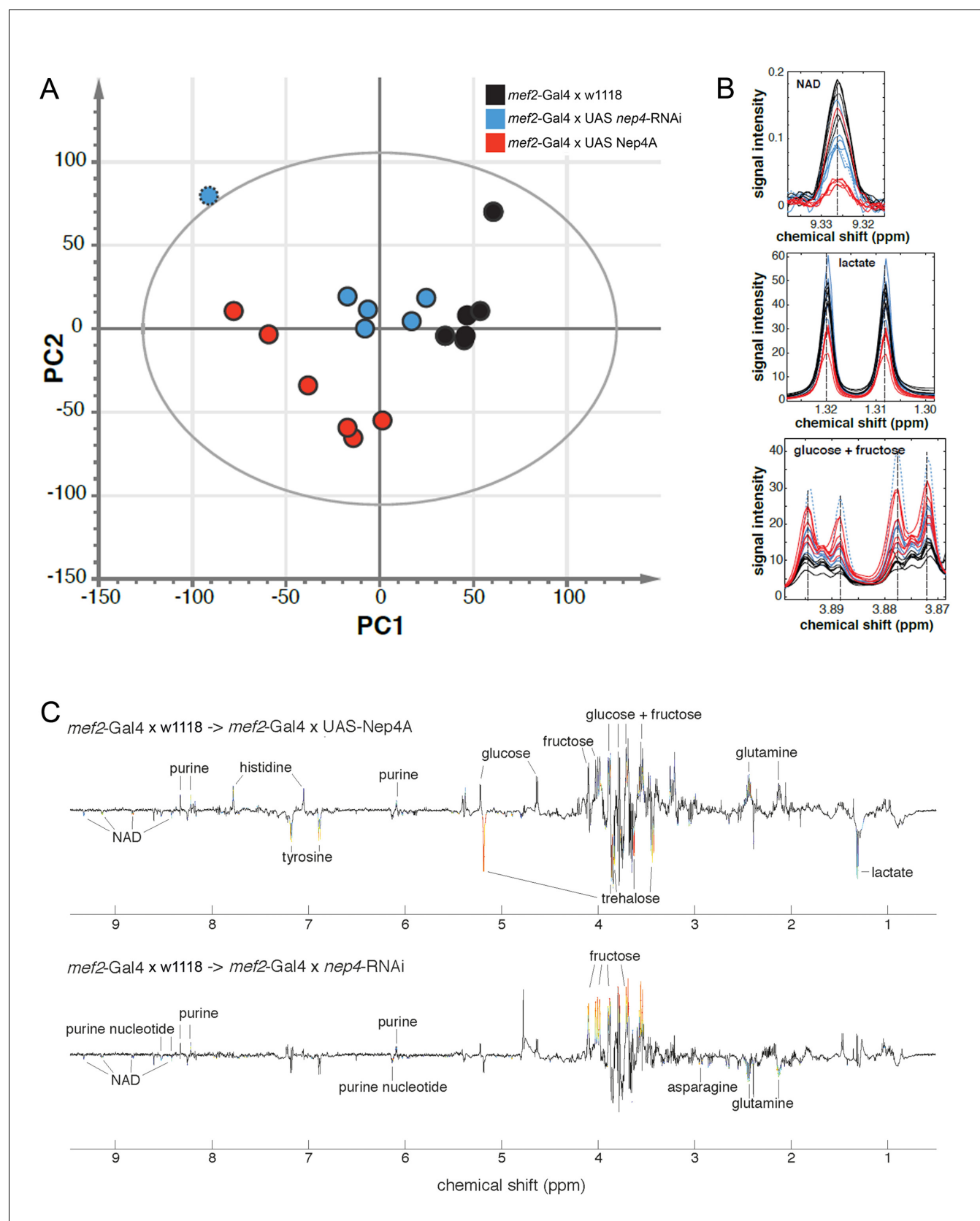


**Figure 2.** Muscle-specific modulation of *nep4* expression affects the metabolite composition in transgenic third instar larvae. **(A)** Score plot based on genotype-specific NMR spectra. PCA score plot showing the scores of six biological replicates for each genotype. Principal component analysis (PCA) Figure 2 continued on next page



## Figure 2 continued

was applied to identify metabolite changes in response to muscle-specific Nep4A overexpression (*mef2*-Gal4 x UAS-Nep4A; red) or knockdown (*mef2*-Gal4 x UAS *nep4*-RNAi; blue), relative to control animals (*mef2*-Gal4 x w<sup>1118</sup>; black). The score plot reveals genotype-specific clustering and thus distinct metabolite compositions in corresponding animals. One *nep4* knockdown sample was distinctly different from the other five. The outlier is marked by a dotted border and was excluded from OPLS-DA identification of significantly affected metabolites. (B) Examples of NMR signals from significantly affected metabolites. Evaluation of the dataset revealed that Nep4A overexpression significantly reduced NAD and lactate concentrations, while glucose and fructose levels were elevated in the same animals. The effects of *nep4* knockdown were less severe; NAD was reduced, and fructose was slightly elevated, compared to levels in control animals. The coloring is the same as in A. The knockdown outlier is marked by a dotted line. (C) OPLS-DA loading plots summarizing the NMR spectral changes induced by *nep4* overexpression and knockdown. Depicted is an overview of the metabolomic changes induced by modifying the expression of *nep4*. Positive and negative signals represent increases and decreases in metabolite concentrations, respectively. Significant alterations are color-coded from blue to red. Red represents the highest correlation between metabolite and genotype.

DOI: [10.7554/eLife.19430.006](https://doi.org/10.7554/eLife.19430.006)

The following source data is available for figure 2:

**Source data 1.** Chemical shifts and detected changes of significantly affected metabolites.

DOI: [10.7554/eLife.19430.007](https://doi.org/10.7554/eLife.19430.007)

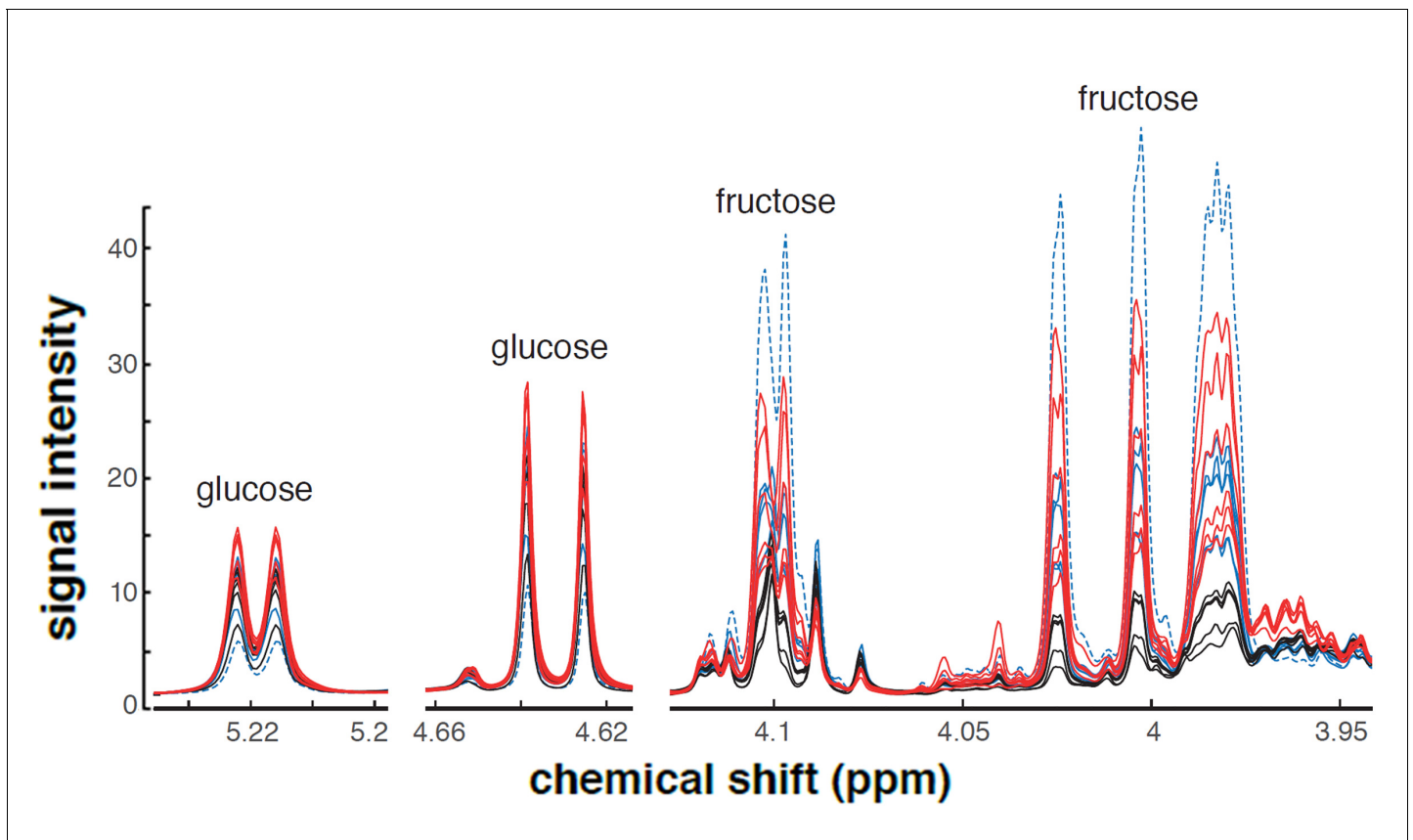


**Figure 2—figure supplement 1.** NMR-spectra of glucose and fructose. The depicted spectra are specific to either glucose or fructose. Signals with contributions from both sugars are excluded. The individual spectra indicate increased levels of both monosaccharides in response to muscle-specific Nep4A overexpression (*mef2-Gal4 x UAS-Nep4A*; red), relative to control animals (*mef2-Gal4 x w1118*; black). The effects of *nep4* knockdown (*mef2-Gal4 x UAS nep4-RNAi*) are depicted in blue. One *nep4* knockdown sample was distinctly different from the other five. The outlier is marked by a dotted line and was excluded from further analysis.

DOI: [10.7554/eLife.19430.008](https://doi.org/10.7554/eLife.19430.008)

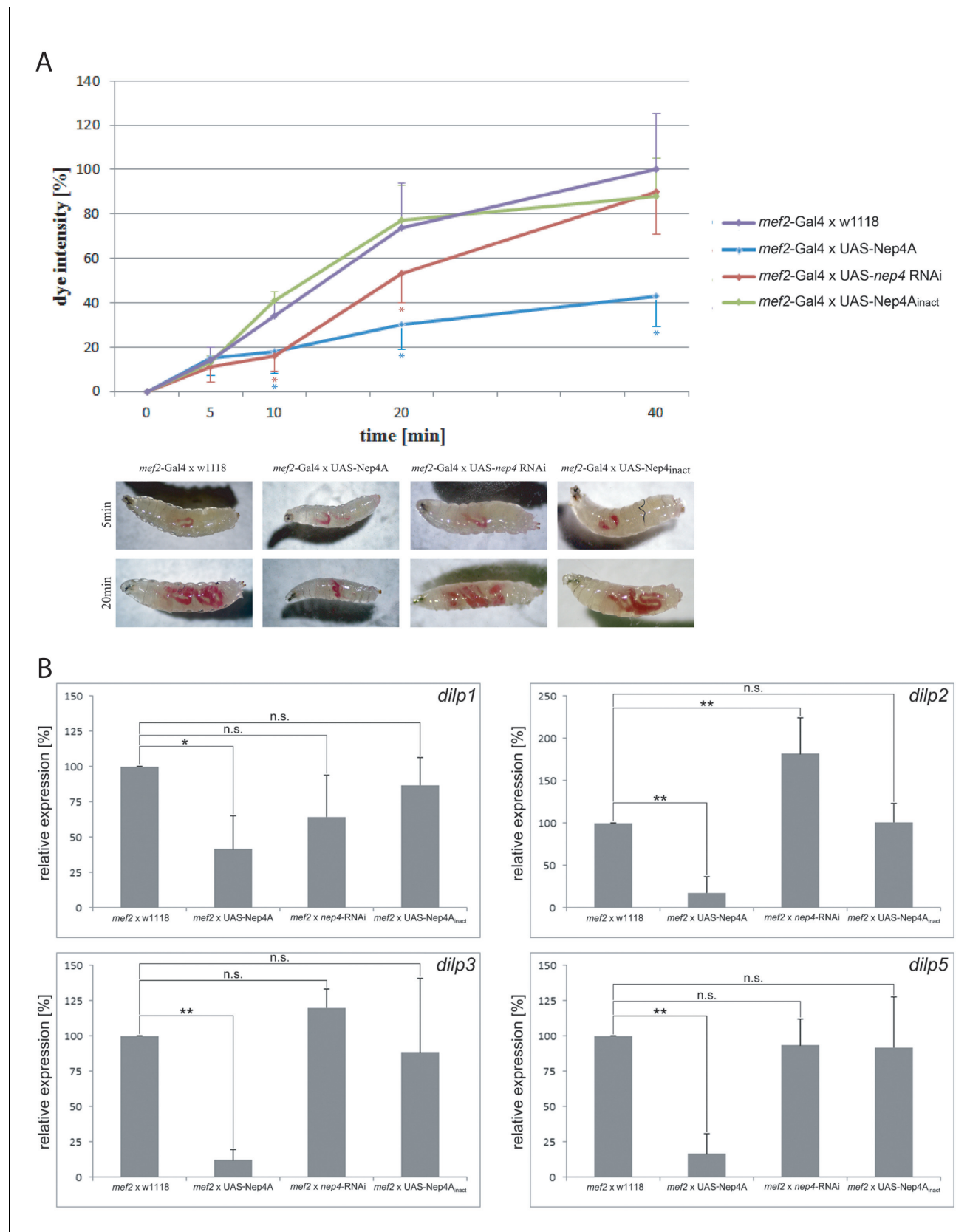


**Figure 3.** Muscle-specific modulation of *nep4* expression affects food intake and *dilp* expression in transgenic third instar larvae. **(A)** The genotype-specific rates of food intake are depicted as percentages (%) relative to the intake in control specimens (*mef2-Gal4 x w1118*) after 40 min of feeding, Figure 3 continued on next page

## Figure 3 continued

which was set to 100%. While *nep4* knockdown animals (*mef2*-Gal4 x UAS-*nep4* RNAi) exhibited reduced food intake after 10 and 20 min of feeding, Nep4A overexpression animals (*mef2*-Gal4 x UAS-Nep4A) were characterized by reduced intake throughout the whole measurement (up to 40 min). Animals overexpressing catalytically inactive Nep4A (*mef2*-Gal4 x UAS-Nep4A<sub>inact</sub>) did not exhibit any significant changes in food intake, when compared to controls. Values represent the mean ( $\pm$  s.d.) of at least six independent biological replicates. Asterisks indicate statistically significant deviations from controls (\* $p$ <0.05, one-way ANOVA with pairwise comparisons). The lower panel depicts representative images of the genotype-specific food intake at the indicated time points. (B) Changes in the expression of selected *dilp* genes are presented as percentages (%) relative to expression in control specimens (*mef2*-Gal4 x w1118), which was set to 100%. Muscle-specific overexpression of Nep4A (*mef2* x UAS-Nep4A) reduced the expression of every *dilp* gene analyzed, while *nep4* knockdown in the same tissue (*mef2* x *nep4*-RNAi) resulted in upregulation of *dilp2*. Animals overexpressing catalytically inactive Nep4A (*mef2* x UAS-Nep4A<sub>inact</sub>) did not exhibit any significant changes in *dilp* expression, when compared to controls. Values represent the mean ( $\pm$  s.d.) of at least three independent biological replicates, each consisting of at least three technical replicates. Asterisks indicate statistical significance (\* $p$ <0.1; \*\* $p$ <0.05, one-way ANOVA with pairwise comparisons); n.s. indicates 'not significant'.

DOI: [10.7554/eLife.19430.009](https://doi.org/10.7554/eLife.19430.009)

The following source data is available for figure 3:

**Source data 1.** Feeding assay.

DOI: [10.7554/eLife.19430.010](https://doi.org/10.7554/eLife.19430.010)

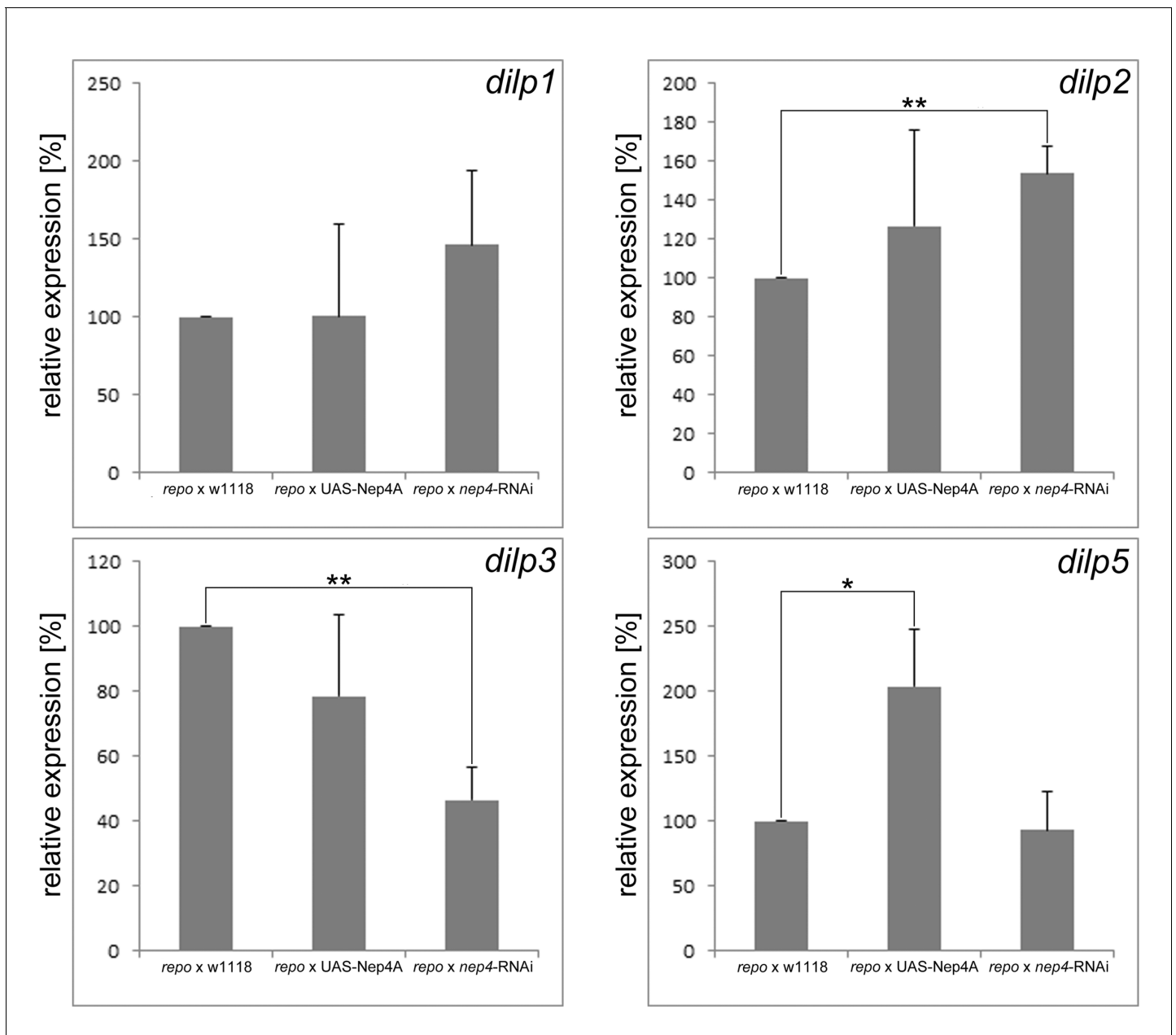


**Figure 3—figure supplement 1.** Glial cell-specific modulation of *nep4* expression affects *dilp* expression in transgenic third instar larvae. Changes in the expression of *dilp* genes are depicted as percentages (%) relative to the expression in control specimens (*repo*-Gal4 x w1118), which was set to 100%. Glial cell-specific overexpression of Nep4A (*repo*-Gal4 x UAS-Nep4A) increased the expression of *dilp5* by 104%, while *nep4* knockdown in the same tissue (*repo* x *nep4*-RNAi) resulted in the upregulation of *dilp2* by 54% and downregulation of *dilp3* by 54%. Values represent the mean (+ s.d.) of at least three independent biological replicates, each consisting of at least three technical replicates. Asterisks indicate statistically significant differences (\*p<0.1; \*\*p<0.05, one-way ANOVA with pairwise comparisons).

DOI: [10.7554/eLife.19430.011](https://doi.org/10.7554/eLife.19430.011)

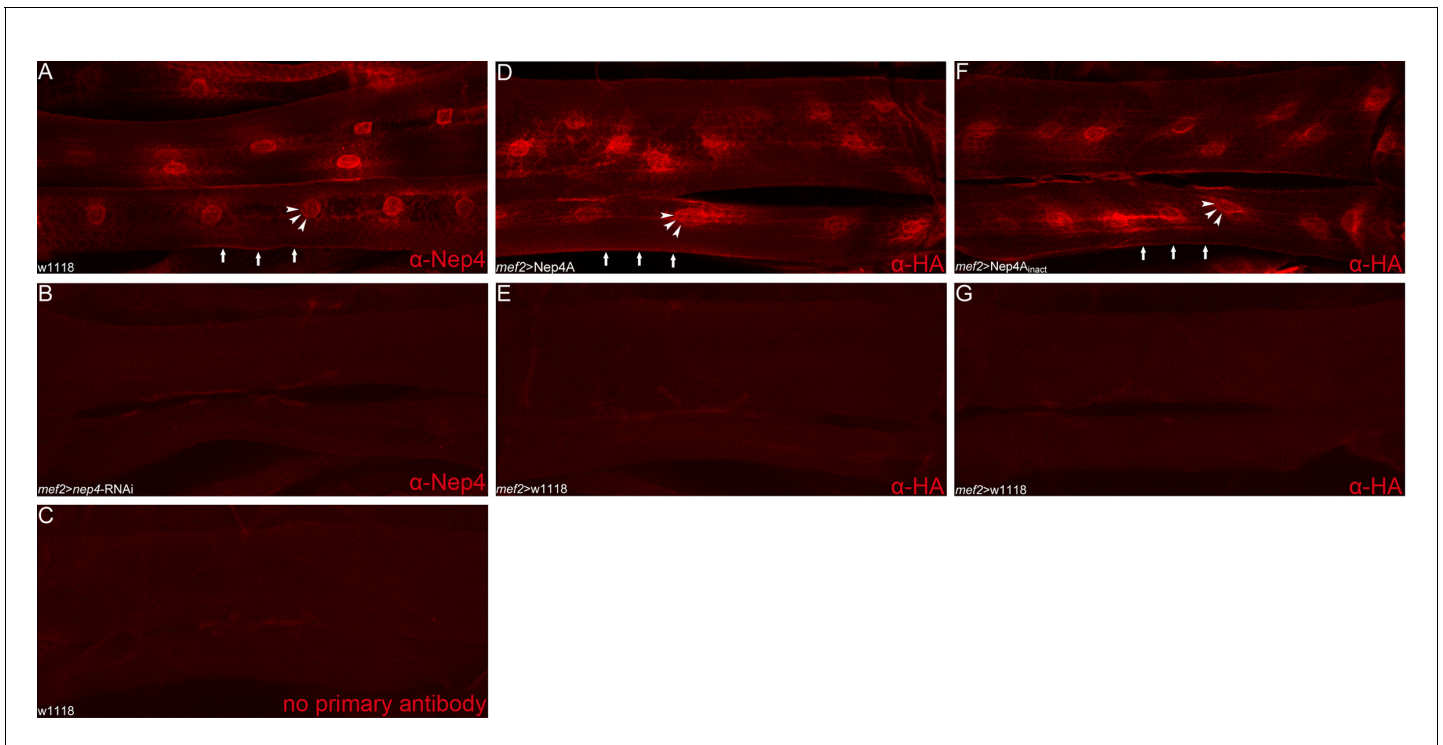


**Figure 4.** Nep4 localizes to the surface of muscle cells. (A) Nep4 protein was labeled with a monospecific antibody (red). In addition to membranes continuous with the nuclear membrane (arrowheads), Nep4 accumulated at the surface of body wall muscles (arrows). (D, F) Nep4 overexpression constructs (*mef2>Nep4A*, *mef2>Nep4A<sub>inact</sub>*) exhibited subcellular localizations identical to that of the endogenous protein. The corresponding constructs were labeled with antibodies detecting the fused HA-tag. (B, C, E, G) Control stainings did not produce any signal above background.

DOI: [10.7554/eLife.19430.012](https://doi.org/10.7554/eLife.19430.012)



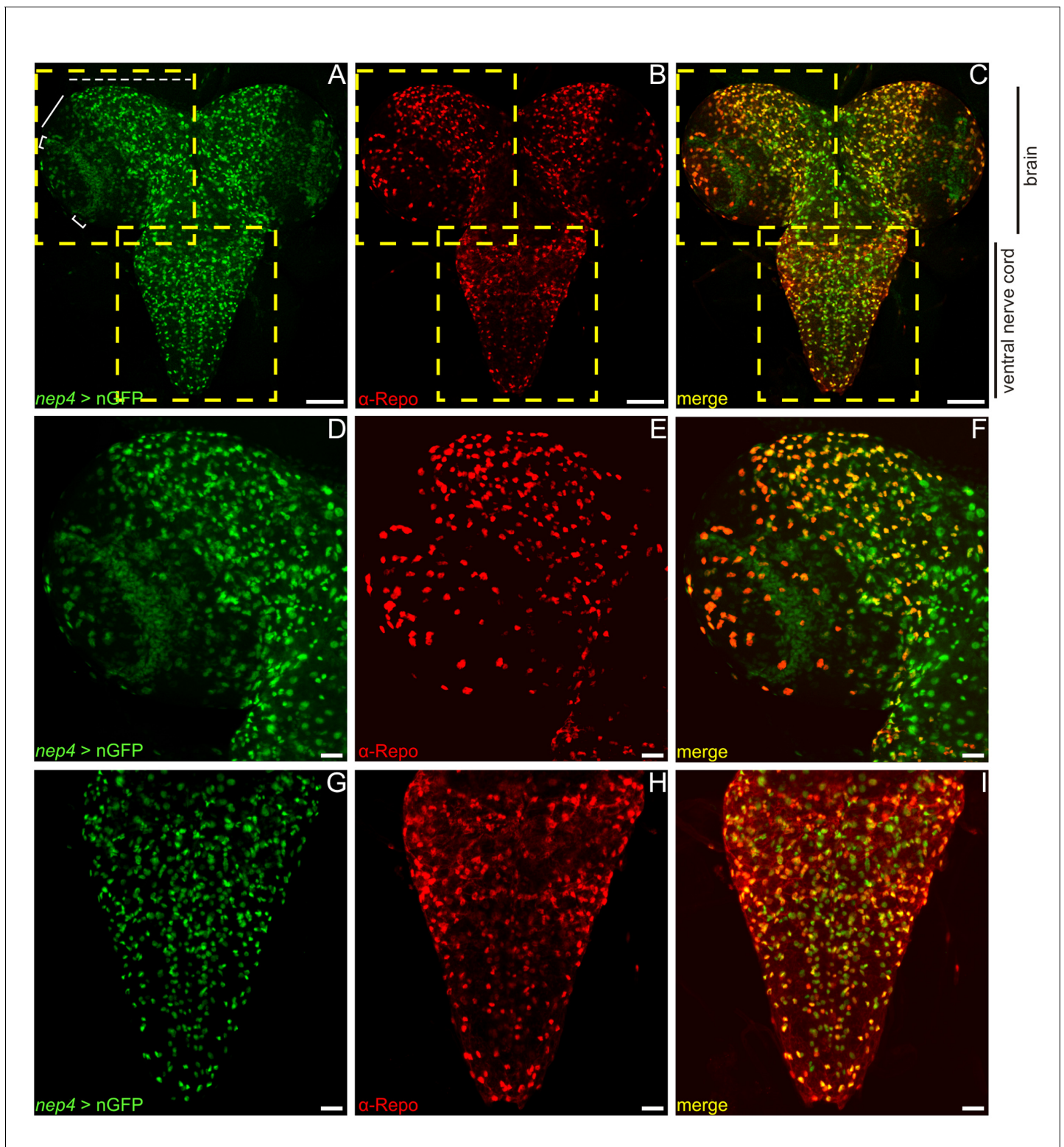


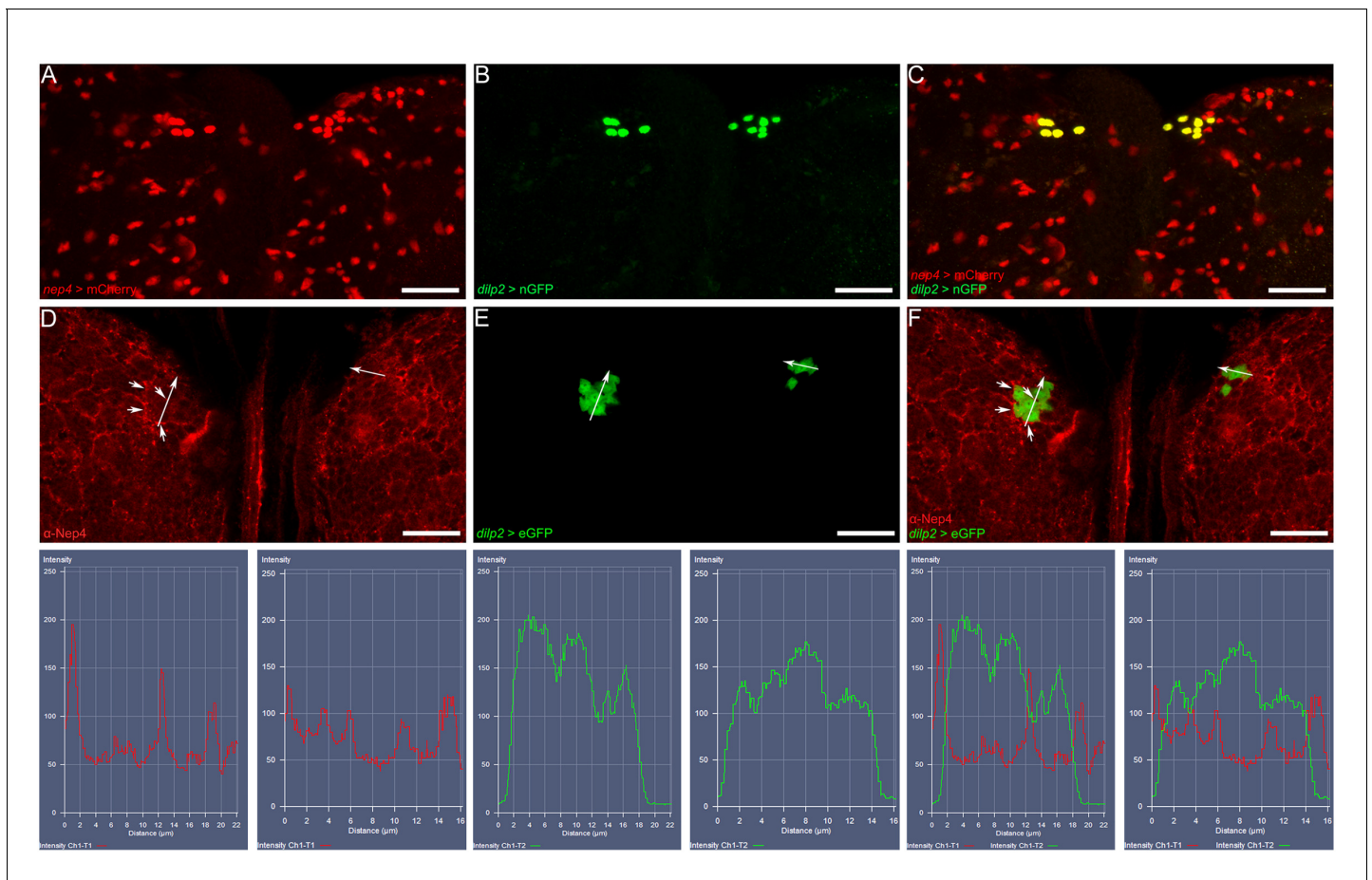
**Figure 5.** *Nep4* is expressed in glial cells and neurons in the central nervous system. *nep4* expression was visualized using a reporter construct that drives nuclear GFP (nGFP) expression in a *nep4*-specific manner (*nep4 > nGFP*, green). Reversed polarity protein was labeled with a monospecific antibody ( $\alpha$ -Repo, red). (A–C) Optical projections of third instar larval whole brain-ventral nerve cord complexes. Scale bars: 100  $\mu$ m; dorsal view, anterior up. Boxes indicate areas of higher magnification, as depicted in (D–F) and (G–I). Within the brain, *nep4* expression was strongest in the central brain (A, dashed line) and in lamina cells (A, brackets), while only few *nep4*-positive medulla cells were observed (A, bar). Within the ventral nerve cord, *Figure 5 continued on next page*

*Figure 5 continued*

*nep4* was expressed in numerous cells along all segments. (D–I) Optical projections of third instar larval brain hemisphere (D–F) and ventral nerve cord (G–I). Scale bars: 20  $\mu$ m; dorsal view, anterior up, midline to right. *nep4* expression colocalized extensively with anti-Repo staining.

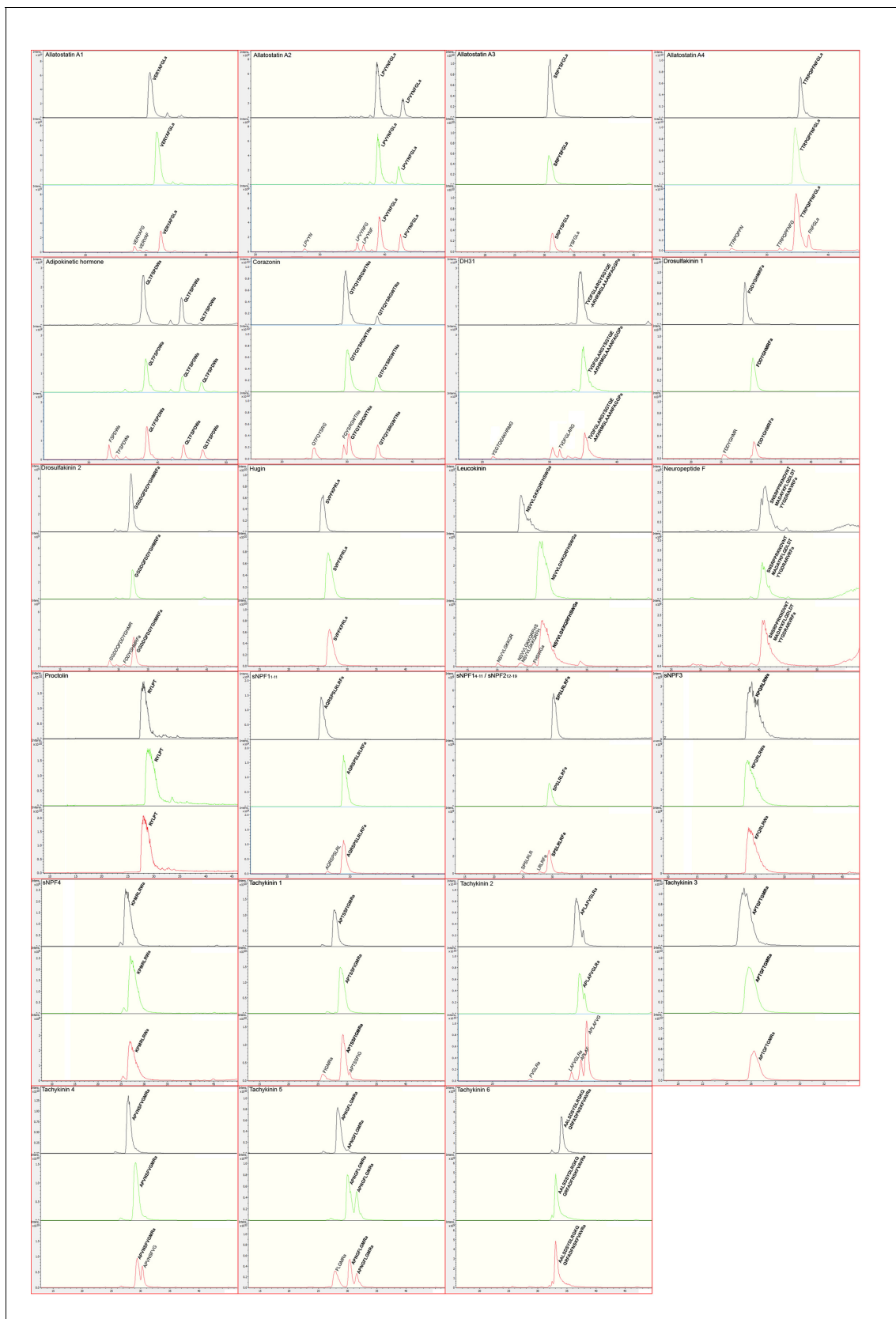
DOI: [10.7554/eLife.19430.013](https://doi.org/10.7554/eLife.19430.013)





**Figure 6.** Nep4 localizes to the surface of insulin-producing cells. (A–C) *nep4* expression was assessed using a reporter line that drives nuclear mCherry expression in a *nep4*-specific manner (*nep4* > mCherry, red). *dilp2* expression was visualized using a reporter construct that drives nuclear GFP expression in a *dilp2*-specific manner (*dilp2* > nGFP, green). Depicted are optical sections (10  $\mu$ m) of a third instar larval central brain. Scale bars: 20  $\mu$ m; dorsal view, anterior up. *nep4* and *dilp2* expression colocalized in IPCs. (D–F) Nep4 protein was labeled with a monospecific antibody (red), and *dilp2* expression was visualized using an eGFP reporter line (*dilp2* > eGFP, green). Depicted are optical sections (10  $\mu$ m) of a third instar larval central brain. Scale bars: 20  $\mu$ m; dorsal view, anterior up. Nep4 accumulated at the surface of numerous cells, including IPCs (D, F, arrowheads). The subcellular localization was assessed with fluorescence intensity measurements (lower panel). The respective regions of evaluation are marked (arrows in D–F).

DOI: [10.7554/eLife.19430.014](https://doi.org/10.7554/eLife.19430.014)



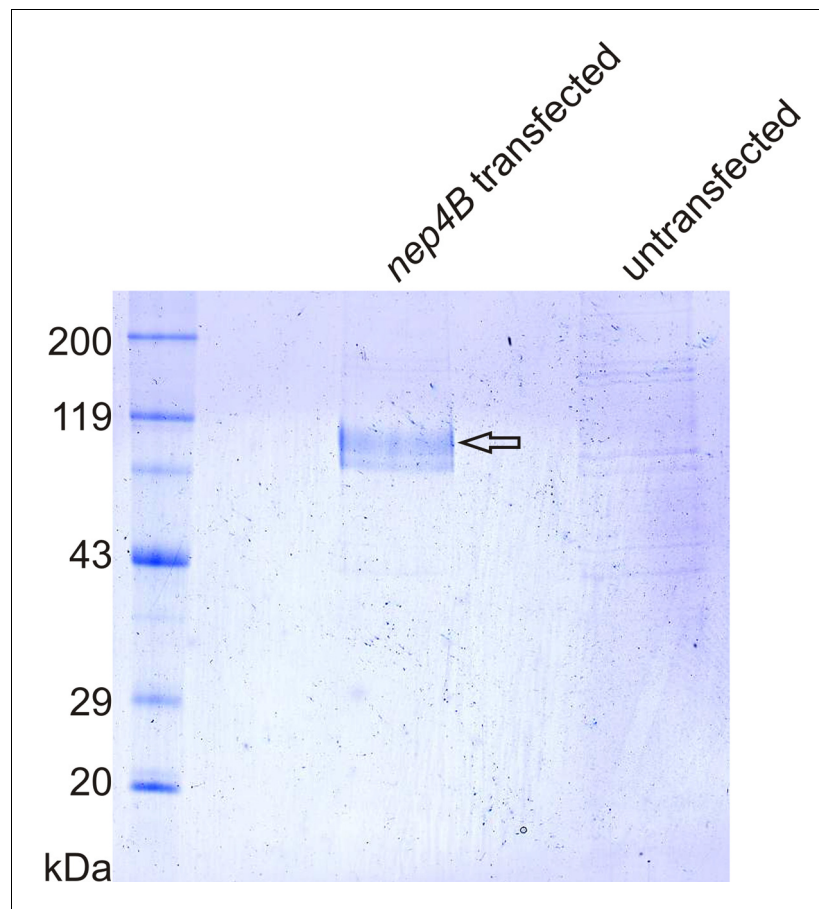
**Figure 7.** Nep4 catalyzes the hydrolysis of peptides that regulate *dilp* expression or feeding behavior. Base peak all MS chromatograms of analyzed peptides. The respective sequences of unprocessed full-length peptides (bold) and of identified Nep4-specific cleavage products are indicated.

Figure 7 continued on next page

*Figure 7 continued*

Unlabeled peaks were not identified. Spectra corresponding to untreated peptides are indicated in black, spectra corresponding to peptides incubated with control preparations lacking Nep4B are indicated in green, and spectra corresponding to peptides incubated with Nep4B-containing preparations are indicated in red. X-axes depict retention time (min).

DOI: [10.7554/eLife.19430.015](https://doi.org/10.7554/eLife.19430.015)



**Figure 7—figure supplement 1.** Heterologously expressed Nep4B can be purified to homogeneity. Coomassie-stained SDS-polyacrylamide gel of Ni-NTA elution fractions. Nep4B (approx. 113 kDa) was efficiently purified from whole cell lysates of *nep4B*-transfected SF21 cells (arrow). In identically treated samples from untransfected control cells, only background binding is apparent.

DOI: [10.7554/eLife.19430.016](https://doi.org/10.7554/eLife.19430.016)